

## Numerical simulation of the dynamic turbulent flow field through a channel provided with baffles: comparative study between two models of baffles: transverse plane and trapezoidal

H. Benzenine<sup>1\*</sup>, R. Saim<sup>2</sup>, S. Abboudi<sup>3</sup> and O. Imine<sup>1</sup>

<sup>1</sup> Département de Génie Mécanique, Faculté de Génie Mécanique,  
Université des Sciences et de la Technologie, 'USTO'  
B.P. 1505 El M'Naouar, 31000 Oran, Algérie

<sup>2</sup> Unité de Recherche des Matériaux et Energies Renouvelables, 'URMER'  
Université Abou Bekr Belkaid, B.P. 119, 13000 Tlemcen, Algérie

<sup>3</sup> Laboratoire Systèmes et Transports, Université de Technologie  
de Belfort-Montbéliard, 'UTBM', Site de Sévenans, 90010 Belfort, France

(reçu le 12 Mai 2010 – accepté le 28 Décembre 2010)

**Résumé** – Une contribution à l'étude numérique d'un écoulement turbulent d'air en présence des chicanes transversales a été menée. Deux différentes formes de chicanes rectangulaire plane et trapézoïdale, disposées en chevauchement dans une conduite de section rectangulaire est présentée dans cet article. Les équations gouvernantes, basées sur le modèle  $k - \varepsilon$  à bas nombre de Reynolds employé pour modéliser la turbulence, sont résolues par la méthode des volumes finis à l'aide de l'utilisation de l'algorithme SIMPLEC. Les profils de vitesse ont été obtenus pour toute la géométrie considérée et pour différentes sections choisis, à savoir, en amont, en aval et entre les deux chicanes, ainsi que les coefficients de frottement ont été obtenues pour différentes sections et pour différents nombres de Reynolds.

**Abstract** - A numerical study turbulent airflow in the presence of transverse baffles was conducted. Two different types of baffles flat rectangular and trapezoidal, arranged in overlapping in a pipe of rectangular section is presented in this article. The governing equations based on  $k - \varepsilon$  model at low Reynolds number used to describe the turbulence phenomena, are solved by the finite volume method using the algorithm SIMPLEC. The velocity profiles were obtained for all the geometry considered and selected for different sections, namely, upstream, downstream and between the two baffles and the friction coefficients were obtained for different sections and for different Reynolds numbers.

**Key word:** Turbulent flow - Plane baffle - Trapezoidal baffle - Finite volume method.

### 1. INTRODUCTION

Turbulent flow in complex geometries receives considerable attention due to its importance in many engineering applications and has been the subject of interest for many researchers. Some of these include the energy conversion systems found in same design of nuclear reactor, heat exchangers, solar collectors and cooling of industrial machines and electronic components.

Considerable work has been done, in recent years, on the investigations of the flow and heat transfer processes at the shell-side are of special interest in order to improve the accuracy of prediction of heat exchangers performances. Some works are of

---

\* b.hamidou@yahoo.fr

particular interest in the improvement and the prediction of the flows around baffles. These studies are devised as well experimental and numerical techniques. An extensive experimental studies of turbulent flow and heat transfer past baffles in heat exchangers has been performed by various authors.

Rajendra *et al.* (2005) where conducted an experimental work on study of heat transfer and friction in rectangular ducts with baffles (solid or perforated) attached to one of the broad walls. The Reynolds number of the study ranges from 2850 to 11500. The baffled wall of the duct is uniformly heated while the remaining three walls are insulated. These boundary conditions correspond closely to those found in solar air heaters.

Over the range of the study, the Nusselt number for the solid baffles is higher than that for the smooth duct, while for the perforated baffles. The friction factor for the solid baffles is found to be 9.6-11.1 times of the smooth duct, which decreased significantly for the perforated baffles with the increase in the open area ratio.

Performance comparison with the smooth duct at equal pumping power shows that the baffles with the highest open area ratio give the best performance. Another experimental study conducted by Wilfried *et al.* (1994). These authors examined experimentally turbulent flows throughout tubular heat exchangers.

The investigators focused on the impact of the baffles on heat transfer, and the geometrical properties of the heat-exchanger on the overall thermal efficiency. Kang-Hoon *et al.* (2003) have experimentally determined the mean heat transfer coefficients in a rectangular channel with porous obstacles. One important result from this work is that the use of baffles improved the thermal efficiency by 300 %, compared with the case in which no baffles were used.

Thermal and hydrodynamic parameters were examined numerically and experimentally by Yong-Gang Lei *et al.* (2008) for a flow passing through a channel with only one helicoidal baffle. A comparative study between three different channels was conducted by the investigators. In the first case, a channel without any baffles was examined. In the second case, the same channel with only one helicoidal baffle was examined. In the third case, the same channel with two helicoidal baffles was examined.

Ahmet *et al.* (2006) examined the effect of the geometric parameters on the steady turbulent flow passing through a pipe with baffles. The effect of the orientation and the distance between nine baffles on the improvement of heat transfer was highlighted in this work.

Another experimental investigation was carried out by Molki *et al.* (1989) to evaluate heat transfer and pressure losses in a rectangular channel with baffles. The authors concluded that baffles raise the pressure losses and the coefficient of heat transfer as well. An investigation of the thermo hydraulic parameters in a rectangular channel heated up by means of fins perforated to different heights is reported by Rajendra *et al.* (2009).

Demartini *et al.* (2004) investigated air flow through a rectangular channel with two plate baffles. A comprehensive analysis of the velocity profiles and pressure gradients was carried out in this work. While Demartini's approach used a rectangular channel with plate baffles, the question remains whether baffles of different shapes will achieve the same results.

The objective of this work is to examine the dynamic behaviour of a turbulent air flow passing through a rectangular channel, containing two baffles attached in

overlapping in the two walls of channel. A comparative study between two various shapes of baffles was approached to know a plate and trapezoidal form.

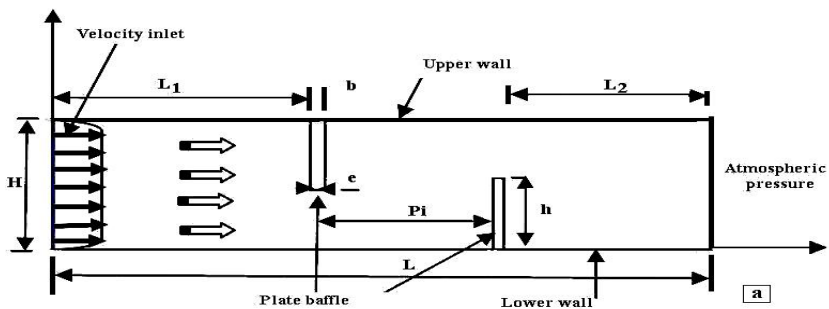
The analysis of the turbulent flow of air in this channel allows comprehension of the dynamic compartment in different sections from a channel to knowing upstream downstream and between the two baffles. For different Reynolds numbers, coefficients of pressure and velocity profiles are presented. The simulation results are then analyzed to explain the aerodynamic phenomena occurring in the system.

## 2. MATHEMATICAL FORMULATION

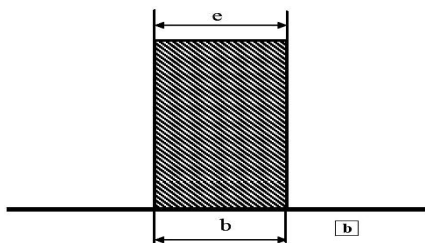
### 2.1 Problem statement

The geometry of the problem is presented on Fig. 1-a, -b and -c. The system consists of air flow moving through a rectangular channel provided with two baffles. Two different forms of baffles are analyzed, a first form is plate baffle (Fig. 1-b) and a second form baffle is trapezoidal (Fig. 1-c). The flow is assumed to be steady and turbulent. In this numerical investigation, the following hypotheses are adopted:

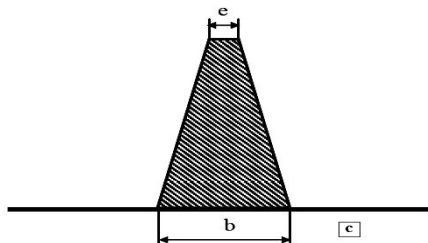
- (i) Physical properties of air are constant.
- (ii) A profile of velocity is uniform at the inlet.
- (iii) The radiation heat transfer is negligible.
- (iv) The flow is assumed to be steady.



a- Schematic of the problem



b- Plate baffle ( $e/b=1$ )



c- Trapezoidal baffle ( $e/b=0.25$ )

Fig. 1: The geometry of the system under investigation

### 2.2 Governing equations

Under these conditions, transport equations that describe the principle of conservation of matter and momentum can be written in the following form Patankar (1974):

$$\frac{\partial}{\partial x}(\rho u \phi) + \frac{\partial}{\partial y}(\rho v \phi) = \frac{\partial}{\partial x} \left[ \Gamma_{\phi} \frac{\partial \phi}{\partial x} \right] + \frac{\partial}{\partial y} \left[ \Gamma_{\phi} \frac{\partial \phi}{\partial y} \right] + S_{\phi} \quad (1)$$

$\phi$  is a vector composed of the scalars  $u$ ,  $v$ ,  $k$  and  $\varepsilon$ .

$u$  and  $v$  stand for the mean velocities towards the axis  $x$  and  $y$  respectively.

$k$  and  $\varepsilon$  stand for kinetic energy and turbulent dissipation respectively.

$\Gamma_{\phi}$  and  $S_{\phi}$  represent the coefficient of turbulent diffusion and the source term associated with the variable  $\phi$  in this order.

The expressions for  $\phi$ ,  $\Gamma_{\phi}$  and  $S_{\phi}$  are presented.

#### Continuity equation

$$\phi = 1 \quad (2)$$

$$\Gamma_{\phi} = 0 \quad (3)$$

$$S_{\phi} = 0 \quad (4)$$

#### Momentum equation in X-direction

$$\phi = u \quad (5)$$

$$\Gamma_{\phi} = \mu_e \quad (6)$$

$$S_{\phi} = \frac{\partial p}{\partial x} + \frac{\partial}{\partial x} \left[ \mu_e \left( \frac{\partial u}{\partial x} \right) \right] + \frac{\partial}{\partial y} \left[ \mu_e \left( \frac{\partial v}{\partial x} \right) \right] \quad (7)$$

#### Momentum equation in Y-direction

$$\phi = v \quad (8)$$

$$\Gamma_{\phi} = \mu_e \quad (9)$$

$$S_{\phi} = \frac{\partial p}{\partial y} + \frac{\partial}{\partial x} \left[ \mu_e \left( \frac{\partial u}{\partial y} \right) \right] + \frac{\partial}{\partial y} \left[ \mu_e \left( \frac{\partial v}{\partial y} \right) \right] \quad (10)$$

#### Turbulent energy equation

$$\phi = k \quad (11)$$

$$\Gamma_{\phi} = \mu_e + \frac{\mu_t}{\sigma_k} \quad (12)$$

$$S_{\phi} = -\rho \times \varepsilon + G \quad (13)$$

#### Turbulent dissipation equation

$$\phi = \varepsilon \quad (14)$$

$$\Gamma_{\phi} = \mu_e + \frac{\mu_t}{\sigma_{\varepsilon}} \quad (15)$$

$$S_{\phi} = (C_1 f_1 G - C_1 f_1 \rho \varepsilon) \frac{\varepsilon}{k} \quad (16)$$

Avec

$$G = \mu_1 \left\{ 2 \left( \frac{\partial \mathbf{u}}{\partial x} \right)^2 + 2 \left( \frac{\partial \mathbf{v}}{\partial y} \right)^2 + \left( \frac{\partial \mathbf{v}}{\partial x} + \frac{\partial \mathbf{u}}{\partial y} \right)^2 \right\} \quad (17)$$

$$\mu_e = \mu_l + \mu_t \quad (18)$$

$$\mu_t = f_\mu \cdot \rho \cdot C_\mu \cdot \frac{k^2}{\varepsilon} \quad (19)$$

The turbulent constants correspond to those suggested by (Launder *et al.* 1974) and (Chiang *et al.* 1980).

These constants are arranged in the table below (**Table 1**)

**Table 1:** Turbulent constant in the governing equations

$C_\mu$	$C_1 = C_3$	$C_2$	$\sigma_k$	$\sigma_\varepsilon$
0.09	1.44	1.92	1	1.3

### Low-Reynolds number $k-\varepsilon$ model

In the version of (Versteeg *et al.* 1995), the modeling damping functions  $f_1$ ,  $f_2$  and  $f_\mu$  used for the (LRN)  $k-\varepsilon$  model are presented as:

$$f_\mu = \left( 1 - \exp(-0.00165 \cdot R_y) \right)^2 \times (1 + 20.5 / R_T) \quad (20)$$

$$f_1 = 1 + (0.05 / f_\mu)^3 \quad (21)$$

$$f_2 = 1 - \exp(-R_T^2) \quad (22)$$

Where:

$$R_T = \frac{\rho \cdot k^2}{\varepsilon \cdot \mu} \quad \text{and} \quad R_y = \frac{\rho \cdot \sqrt{k} \cdot y}{\mu} \quad (23)$$

The damping function ( $f_\mu$ ), which is a function of dimensionless wall-normal distance  $R_y = y^+ = y\sqrt{k}/n$ , is used to model the damping effect associated with pressure-strain correlations in the vicinity of walls.

### **2.3 Boundary conditions**

A fully developed turbulent flow is considered. The quantities  $U$ ,  $k$ ,  $\varepsilon$  are obtained by using numerical calculations based on the  $k-\varepsilon$  model for low Reynolds Number.

The boundary conditions are listed below:

1- At the inlet of the channel:

$$\mathbf{u} = U_{in}, \quad \mathbf{v} = 0 \quad (24)$$

$$k_{in} = 0.005 U_{in}^2 \quad (25)$$

$$\varepsilon_{\text{in}} = 0.1 k_{\text{in}}^2 \quad (26)$$

$k_{\text{in}}$  stands for the admission condition for turbulent kinetic energy, and  $\varepsilon_{\text{in}}$  is the inlet condition for dissipation.

2- At the walls:

$$u = v = 0 \quad (27)$$

$$k = \varepsilon = 0 \quad (28)$$

3- At the exit: all gradients are null.

$$\frac{\partial u}{\partial x} = \frac{\partial v}{\partial x} = \frac{\partial k}{\partial x} = \frac{\partial \varepsilon}{\partial x} = 0 \quad (29)$$

$$P = P_{\text{atm}} \quad (30)$$

The Reynolds number based on hydraulic diameter  $D_H$  is taken according to the experiment of (Endres *et al.* 2001), it is equal to  $Re = 8.73 \times 10^4$ . This adimensional parameter is defined as follows:

$$Re = \frac{\rho \cdot D_H \cdot U_0}{\mu} \quad (31)$$

The expression of coefficient of friction  $f$  is defined as follows:

$$f = \frac{2 \cdot \tau_w}{\rho \cdot U_b^2} \quad (32)$$

where  $\tau_w$  presents the rate of shearing to the wall,  $\rho$  the density and  $U_b$  the average axial speed of the section.

### 3. NUMERICAL RESOLUTION

Numerical simulations were tested by varying the number of elements of calculation. Stability and a convergence of the model reached for all the grids were assured. A non structured grid elements with the quadrilateral type used because it considered being more adequate for the geometry suggested.

The governing equations of our problem are solved by the finite volume method (FVM), based on the algorithm SIMPLEC (Patankar, 1980), for the coupling pressure-velocity. Taking into account the characteristics the flow, the numerical schema Quick of (Patankar, 1980) was applied to the interpolations and a system of second order was used for the terms of pressure.

### 4. RESULTS AND DISCUSSION

The results reported in Demartini's work were achieved experimentally. Demartini *et al.* considered a flat plate baffle. In this work, we investigate the effect of the shape of the baffle on the flow patterns.

A waved baffle is considered, and all the modeling conditions are inspired from the experimental study. Sensitivity analysis of the mesh and the numerical model validation are presented in this section.

#### 4.1 Sensitivity analysis of the mesh

A non-uniform mesh of (195 x 82) in the vertical and horizontal directions proved to be sufficient to model the system. The meshing size is comparatively small near the boundaries and the baffles, so a good estimate of the gradients can be obtained.

Many meshing sizes (  $N_x$ ,  $N_y$  ) were tried. For some number of cells, the result remains almost constant regardless the number of cells (see **Table 2**).

The values in the table indicate the properties at the point  $(x, y) = (0.554, 0.16)$ . The different meshing sizes smaller than the one adopted indicate a difference in Reynolds number of 1.00 % at the same position.

**Table 2:** Dependence of the properties on the meshing size

Grille	195×82	165×62	105×42	75×26
X	0.554	0.554	0.554	0.554
Y	0.16	0.16	0.16	0.16
$\Psi_{\max}$	2.094	2.0938	2.044	2.017
$U_{\max}$	34.406	34.441	33.069	31.863
$V_{\max}$	30.509	30.272	29.808	28.013

**Table 2** shows the various grids used for a Reynolds number equal to  $8.73 \times 10^4$ . The various values the vertical and horizontal velocities as well as the maximum value of the stream function are presented.

#### 4.2 Validation of the model

For the numerical simulations presented in this work, we refer to the experimental work done by (Demartini *et al.* 2004) and (Endres, 2001), who studied the baffles with a plane shape.

The geometric dimensions of the system are listed below:

-length of the channel  $L=0.554$  m ; -height of the channel  $H=0.146$  m ; -thickness of the baffle  $e=0.08$  m ; -distance between baffles  $w=0.142$  m ; -distance between the intake of the channel and the first baffle  $L_1=0.218$  m ; -distance between the second baffle and the exit of the channel  $L_2=0.174$  m ; -hydraulic diameter  $D_H=0.167$  m ; -velocity of air particles at the inlet  $U_{\text{in}}=7.8$  m/s .

Figure 2 and figure 3 shows our results and those obtained by (Demartini *et al.*, 2004). It represents the profiles of velocity at  $x = 0.159$  m and  $x = 0.525$  m respectively.

It is clear from Fig. 3 that the modeling results are in good agreement with the Demartini's experimental results. Even more importantly, it is concluded that the velocity profiles do not depend significantly on the shape of the obstacle.

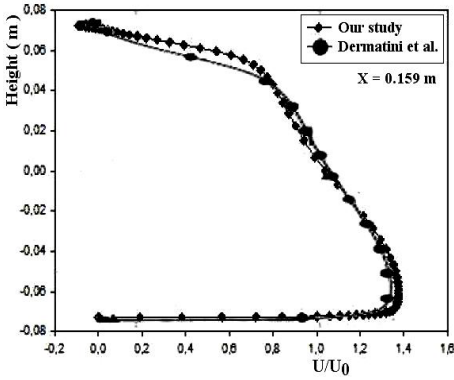


Fig. 2: Comparison between the modeling results and Demartini's results for  $x = 0.159$  m

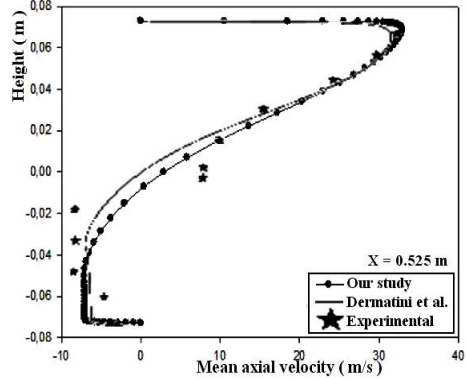


Fig. 3: Comparison between the modelling results and Demartini's and Endres results for  $x = 0.525$  m

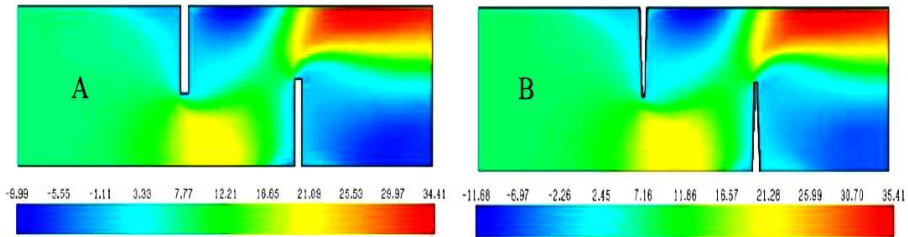


Fig. 4: Axial velocity field in channel for two studied cases (A:  $e/b=1$ , B:  $e/b=0.25$ )

Fig. 4 shows the axial velocity plots for the two cases treated (A) rectangular baffles, (B) trapezoidal baffles at  $Re = 8.73 \times 10^4$ . It indicates clearly that the values of velocity are very low in the vicinity of the two baffles especially in the areas located downstream. This is due to the presence of the zones of recirculation. One notices also the increase velocity in space between the top of each baffle and the walls of the channel.

This increase is generated first of all by the singularity represented by the obstacles, also by the presence of a recycling which then results an abrupt change from the direction of the flow. It is also noticed that the most values velocity appear close the top of the channel with a process of acceleration which starts just after the second baffle.

The variation of velocity for the two cases appears clearly on contours and their scales which present positive and negative values. For studying this dependence well, we plotted the velocity distribution for these sections:  $x=0.159$ ,  $x=0.189$ ,  $x=0.255$ ,  $x=0.285$ ,  $x=0.315$ ,  $x=0.345$  and  $x=0.525$ .

In the two treated cases ( $e/b=0.25$ : trapezoidal) and ( $e/b=1$ : plate), Fig. 5 displays the profiles of velocity upstream the first baffle for two sections:  $x=0.159$  m and  $x=0.189$  m. The presence of the first baffle located in the higher half of the channel induces a strong reduction of velocity, paradoxically in the lower half of channel, where the flow increase and especially in the vicinity of the passage under the baffle. Resulted also show that the use of the one of the two shapes of baffle (rectangular ' $e/b=1$ ' or trapezoidal ' $e/b=0.25$ ') does not influence the dynamic behaviour of the air upstream the first baffle.

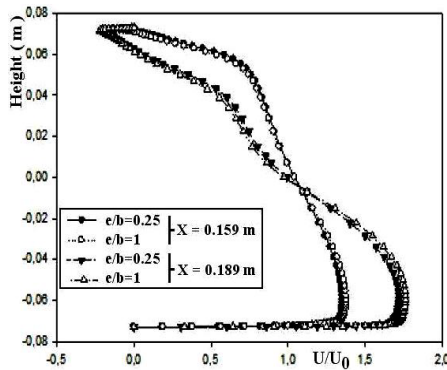


Fig. 5: Profiles of axial velocity upstream of the first baffle for the two treated cases

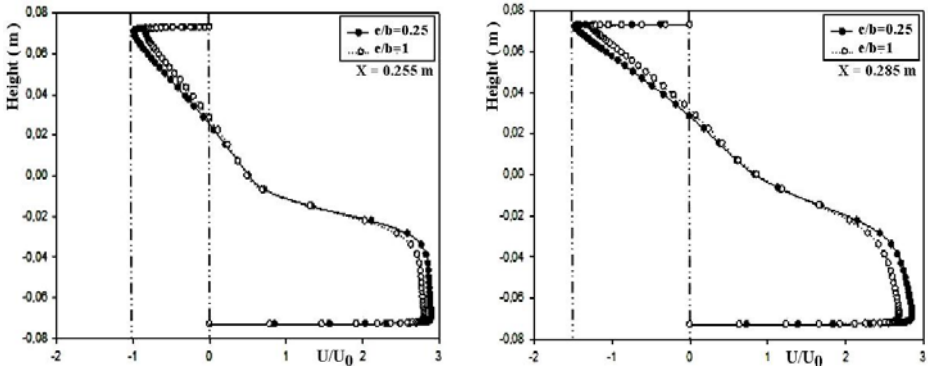


Fig. 6: Profiles velocity enters the first and the second baffle for  $x=0.255$  and  $x=0.285$

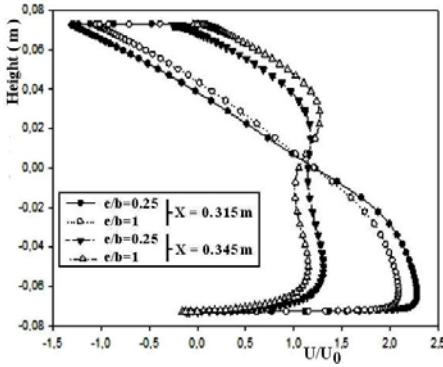


Fig. 7: Profiles velocity upstream of the second baffle

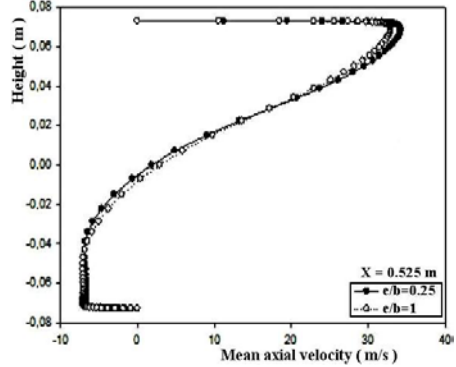


Fig. 8: Profiles velocity at the exit section of the channel

In the intermediate zone, at the position:  $x=0.255\text{ m}$  and  $x=0.285\text{ m}$  of the entry, in Fig. 6, the flow is characterized by very high velocity in the lowest part of the channel. Its size measures almost three times the reference velocity (7.8 m). In the higher part of the channel, negative velocity indicates the presence of the recirculation of the flow behind the first baffle. What was also noticed, the flow in the presence of baffles of trapezoidal forms accelerates more and more left towards the line by increasing the size of the recirculation zone.

For the two configurations of baffles studied ( $e/b=0.25$  and  $e/b=1$ ) and according to the Fig. 7, the adimensional profiles velocity of the flow at distances equal to 0.055 m and 0.025 m before the second baffle, corresponding to positions  $x=0.315\text{ m}$  and  $x=0.345\text{ m}$ , the results show that the flow while approaching the second baffle, its velocity is reduced in the lower part of the channel, while in the higher part is increased, compared to the two preceding sections.

The negative values observed in the numerical results at the location  $x=0.315\text{ m}$  are disappeared at the place  $x=0.345\text{ m}$ . Here the velocity profile is almost null in the lower part of the channel. While in the higher part the air starts again to accelerate towards this breach above the second baffle.

These remarks are valid for the two types of baffles, with these two sections. It was well confirmed that the trapezoidal baffles ensure the increase rate of the flow in the two directions (positive and negative).

To the exit of the channel, for  $x=0.525\text{ m}$  differently say to 29 mm before the exit, the profile of velocity was presented on the Fig. 8. Maximum values axial velocity in the two cases reached more than 4 times of the reference velocity  $U_0$ .

These values are generated because of the strong recirculation of the flow in the back face of the second baffle. It is also noticed that the case  $e/b=0.25$  ensures axial velocities higher than that in the case of  $e/b=1$ .

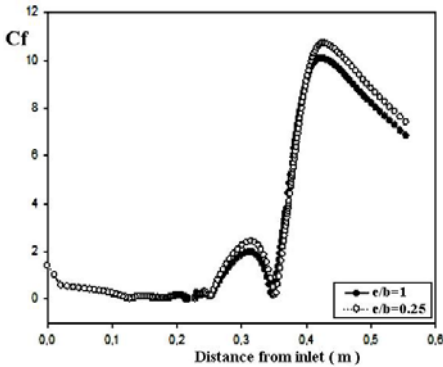


Fig. 9: Variation of coefficient of friction along the higher wall of the channel the two type of baffles

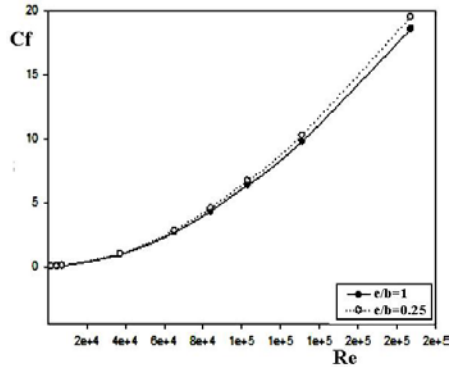


Fig. 10: Variation of coefficient of friction for different Reynolds number

In general, the increase in heat transfer is concerned with the penalty in the terms of coefficient of friction which induces an increase in the pressure drop. The figure 9 shows the variation of the coefficient of friction along the high wall for the two cases. It is noticed that the highest values is in the intermediate zone between the two baffles because the recirculation of the fluid and at the exit.

The latter is caused by the orientation of the flow by the second baffle towards the superior part of the channel with large velocity. For this reason we have presented the evolution of friction in the higher wall. It is also noted that the low values of coefficient of friction locate upstream the first baffle is caused by the absence of the obstacles.

From the point of view forms of baffle, it is interesting to study the influence of Reynolds numbers on the variation of coefficient of friction.

The figure 10 presents this dependence. It is clear the for the two cases ( $e/b = 0.25$  and  $e/b = 1$ ) and for a Reynolds Number going from  $1.87 \times 10^3$  to  $1.87 \times 10^5$ , the increase in this last induced to increase the friction and consequently an pressure drop more considerably after a value of Reynolds equal to  $6,53 \times 10^4$ .

### 5. CONCLUSION

The contribution to the study of a turbulent flow in a rectangular channel provided with the baffles is carried out. The numerical results obtained by the finite volume method, are validated and presented to analyze the dynamic behaviour of a turbulent flow using the model  $k - \epsilon$  with low Reynolds number and for two different forms of baffle (rectangular plane and trapezoidal).

The evolution axial velocity and the coefficient of friction are treated along the channel and for various Reynolds numbers. The use of the baffles of trapezoidal form ensures a considerable increase velocity per contribution the baffles of rectangular form but the only disadvantage east causes with an increase in friction coefficient.

## NOMENCLATURE

$C_1$ : Constant used in the standard $k-\varepsilon$ model	$C_2$ : Constant used in the standard $k-\varepsilon$ model
$C_\mu$ : Constant used in the standard $k-\varepsilon$ model	$f_1, f_2, f_\mu$ : The modelling damping functions used for the (LRN) $k-\varepsilon$ model
$e$ : Width of baffles, m	$H$ : Height of air tunnel in solar collector, m
$k$ : Turbulent kinetic energy, $m^2/s^2$	$h$ : Baffle height, m
$L_1$ : Distance upstream of the first chicane, m	$L$ : Channel length, m
$L_2$ : Distance downstream of the second fin, m	$Pr$ : Laminar Prandtl Number
$P$ : Pressure, Pa	$Pr_t$ : Turbulent Prandtl Number
$P_i$ : Distance between two baffles, m	$Re$ : Number de Reynolds
$R_T, R_y$ : Constant used in (LRN) $k-\varepsilon$ model	$u, v$ : Air velocity in the $x, y$ direction, m/s
$S_\phi$ : Limit of source for the general variable	$U_{in}$ : Inlet velocity, m/s

### Greek Symbols

$\varepsilon$ : Dissipation rate of turbulence energy, $m^2/s$	$\phi$ : Stands for the dependent variables $u, v, k$ and $\varepsilon$
$\mu_l, \mu_t$ : Laminar, turbulent viscosity, Pa.s	$\rho$ : Density of the air, $kg/m^3$
$\mu_e$ : Effective viscosity, Pa.s	$\nu$ : Kinematics viscosity, $pl$
$b$ bulk; $In$ Inlet, outlet of the test section;	<b>Subscripts and Superscripts</b>
$f$ fluid; $s$ solide	$t$ turbulent; $w$ wall;
	$e$ effective;

## REFERENCES

- [1] A. Tandiroglu, 'Effect of Flow Geometry Parameters on Transient Heat Transfer for Turbulent Flow in a Circular Tube With Baffle Inserts', International Journal of Heat and Mass Transfer, Vol.49, N°9-10, pp. 1559 - 1567, 2006.
- [2] C.C. Chieng and B.E. Launder, 'On the Calculation of Turbulent Heat Transport Downstream from an Abrupt Pipe Expansion', Numerical Heat Transfer, Vol. 3, N°2, pp. 189 – 207, 1980.
- [3] L.C. Demartini, H.A. Vielmo and S.V. Möller, 'Numeric and Experimental Analysis of the Turbulent Flow through a Channel With Baffle Plates', Journal of the Brazilian Society of Mechanical Sciences and Engineering, Vol. 26, N°2, pp. 153 – 159, 2004.
- [4] L.A.M. Endres and S.V. Möller, 'On the Fluctuating Wall Pressure Field in Tube Banks', Nuclear Engineering and Design, Vol. 203, N°1, pp. 13 – 26, 2001.
- [5] B.B. Gupta, J.A. Howell, D. Wu and R.W. Field, 'A Helical Baffle For Cross-Flow Micro Filtration', Journal of Membrane Science, Vol. 99, pp. 31 – 42, 1995.
- [6] W.P. Jones and B.E. Launder, 'The Prediction of Laminarization with a Two-Equation Model of Turbulence', International Journal of Heat and Mass Transfer, Vol. 15, N°2, pp. 301 - 314, 1972.
- [7] K. Kang-Hoon and N.K. Anand, 'Use of Porous Baffles to Enhance Heat Transfer in a Rectangular Channel', International Journal of Heat and Mass Transfer, Vol. 46, N°22, pp. 4191 - 4199, 2003.

- [8] B.E. Launder and D.B. Spalding, '*The Numerical Computation of Turbulent Flow*', Computer Methods in Applied Mechanics and Engineering, Vol. 3, N°2, pp. 269 - 289, 1974.
- [9] M. Molki and A.R. Mostoufizadeh, '*Turbulent Heat Transfer in Rectangular Ducts with Repeated-Baffle Blockages*', International Journal of Heat and Mass Transfer, Vol. 32, N°8, pp. 1491 - 1499, 1989.
- [10] S.V. Patankar, '*Numerical Heat Transfer and Fluid Flow*', Hemisphere Publishing Corporation, New York, 1980.
- [11] K. Rajendra, B.K. Maheshwarib and K. Nitin, '*Experimental Study of Heat Transfer Enhancement in an Asymmetrically Heated Rectangular Duct with Perforated Baffles*', International Communications in Heat and Mass Transfer, Vol. 32, N°1-2, pp. 275 - 284, 2005.